Effect of Encapsulation on Phase Transition Temperature of Liposomes. Binding Sites in HSA

Leszek Sułkowski, Joanna Równicka-Zubik, Bartosz Pawełczak, Jadwiga Pożycka & Anna Sułkowska

Published online: 15 Dec 2014.

Submit your article to this journal ⬀

Article views: 23

View related articles ⬀

View Crossmark data ⬀

Effect of Encapsulation on Phase Transition Temperature of Liposomes. Binding Sites in HSA

LESZEK SUŁKOWSKI,[1] JOANNA RÓWNICKA-ZUBIK,[2]
BARTOSZ PAWEŁCZAK,[2] JADWIGA POŻYCKA,[2]
AND ANNA SUŁKOWSKA[2,*]

[1]Department of General and Vascular Surgery with Polytrauma Sub-Department, Regional Specialistic Hospital, Czestochowa, Poland
[2]Medical University of Silesia, Faculty of Pharmacy, Department of Physical Pharmacy, Sosnowiec, Poland

The degree of encapsulation of 5-fluorouracil (5-FU) and vinorelbine (VIN) to dipalmi-toylphosphatidylcholine (DPPC) liposomes was estimated using UV-vis spectroscopy. The phase transition temperature was determined by the differential scanning calorime-try (DSC). 5-FU incorporates in more extend to liposomes than VIN and affects phase transition temperature of phospholipide forming liposomal membrane. There is only a slight influence of VIN on the 5-FU encapsulation in liposome vesicle while 5-FU affects significantly the VIN content in the liposome vesicles. The binding sites of VIN and 5-FU in HSA determined by fluorescence quenching method were confirmed by computer simulation.

Keywords Liposomes; 5-fluorouracil; vinorelbine; phase transition; binding site in HSA

Introduction

Unspecific transport of medicines to the receptors can occur by serum albumin.

Liposomes as drug delivery systems are applied in cancer treatment since it improves efficacy and reduces toxic side effects of the medicines. Pharmacokinetic and efficacy of liposomal vinorelbine system was described in [1]. In the multidrug therapy used in cancer treatment another difficulty appears: encapsulation of two drugs with different affinity to phospholipid membrane.

The aim of this study was to encapsulate 5-fluorouracil and vinorelbine into liposomes in the process of modified reversed phases evaporation (mREV). The drugs are clinically approved. 5-fluorouracil is one of the most commonly used drugs to treat many types of cancer. It may be combined with other anticancer drugs or with radiotherapy. Vinorelbine,

---

Color versions of one or more of the figures in the article can be found online at www.tandfonline.com/gmcl.

cycle-specyfic anticancer agent, is used alone and in combination with other medications to treat certain types of non-small cell lung cancer that has spread to nearby tissues or to other parts of the body [1]. Its antitumor activity relies on inhibition of cell proliferation in late G_2 and M phase. Vinorelbine interacts with tubuline and prevents creation of microtubules [2]. The comparison of temperature of phase transition of liposomes containing drug/s (DPPC/5-FU, DPPC/VIN, DPPOC/5-FU/VIN) with DPPC liposomes should indicate the way of incorporation of the drug within liposomal vesicle. Spectrofluorescence study of the binding of 5-FU and VIN to human serum albumin, being transporting protein of a drug to its receptor, was confirmed by computer simulation. The study should allows us to determine 5-FU and VIN competitive incorporation to liposome vesicle.

Materials and Methods

1. Reagents

To receive liposomal membranes dipalmitoylphosphatidylcholine 99 % (DPPC) [Sigma-Aldrich Chemical Co., Germany]; buffer PBS of pH 7,4 prepared from K_2HPO_4 [Polish Chemical Reagents S.A. POCH Gliwice] and NaH_2PO_4 [Polish Chemical Reagents S.A. POCH Gliwice]; chloroform [Polish Chemical Reagents S.A. POCH Gliwice]; dichloromethan 99 % HPLC [Sigma-Aldrich Chemical Co., Germany]; cholesterol (3β – hydroxy – 5 cholestene 5 – cholesten – 3β – ol) [Sigma-Aldrich Chemical Co., Germany] were used. Human serum albumin fraction V (HSA), crystallized and lyophilized was purchased from MP Biomedicals (France). Vinorelbine ditartrate salt hydrate (5′-noranhydrovinblastine, navelbine tartrate; VIN) and 5-fluorouracil (2,4-dihydroxy-5-fluoropyrimidine; 5-FU) were obtained from Sigma-Aldrich Chemical Co. (Germany).

2. Procedure of preparation of liposomes

Modified reversed phase evaporation method (mREV) [3] was used to obtain liposomes. 2.0 ml of buffer (pH 7.4) and 3.5 ml of organic phase (phospholipid (DPPC) in dichloromethane/chloroform) were put in the preparatory thermostated at 55°C and stirred extensively. After evaporation of organic solvents the obtained liposome emulsion was centrifuged at 10000 rpm to separate liposome from supernatant where un-embedded drugs remained. In this way liposomes (DPPC, DPPC/5-FU, DPPC/VIN, DPPC/VIN/5-FU have been prepared. Molar ratio of DPPC to cholesterol was 4:1. The amount of drugs used separately for each preparation was $4,5 \times 10^{-4}$ mol and for composition of both drugs it was 9×10^{-4} mol. The degree of encapsulation of drug into liposome vesicles DPPC/VIN DPPC/5-FU DPPC/VIN/5-FU, defined as a concentration of VIN and 5-FU in phospholipid carrier, is determined using UV-vis spectroscopy, according to procedure described in [3, 4].

2.1. Differential scanning calorimetry. The DSC study was conducted on differential scanning calorimeter Seteram Micro DSC III with heat flow of Calvet type and cylindrical measurement system within the temperature range 275-335K with heating rate 1.2 Kxmin^{-1}.

3. Spectroscopic studies

3.1. Measuring conditions. All measured solutions were prepared at physiological pH (7.4 ± 0.1) in 0.1 M PBS. Absorption and fluorescent emission spectra were recorded at temperature 23°C, 2 minutes after preparation of the sample.

3.2. Samples preparation. A working solutions of HSA 66 kDa (1.0×10^{-6} M), VIN (1.0×10^{-3} M) and 5-FU (1.0×10^{-3} M) in 0.1 M PBS. The appropriate volumes of HSA solution were transferred to quartz cuvette and titrated by a Hamilton syringe with increasing portions of a VIN or 5-FU. The concentration of HSA in samples was constant at 1.0×10^{-6} M. The final concentration of VIN or 5-FU in HSA solution was in the range from 1.0×10^{-6} to 3.2×10^{-5} M to give ligand:protein molar ratio from 1:1 to 32:1.

3.3. Fluorescence analysis. Fluorescence emission spectra were recorded on a spectroflu-orimeter Jasco FP-630 with a thermostatically controlled cell holder using quartz cells 1 cm × 1 cm × 4 cm. SFM-spectra were visualized in terms of relative fluorescence. Compensation error of apparatus for wavelength (λ) is equal to ± 1 nm and for relative fluorescence (RF) ± 0.01. Two excitation wavelength (λ_{ex}) were chosen to excite fluorophores of HSA. λ_{ex} 295 nm excites the tryptophanyl residue, and λ_{ex} 275 nm excites both tyrosyl and tryptophanyl residues. Emission spectra were recorded within the range from 280 nm to 500 nm and from 305 nm to 500 nm for $\lambda_{ex} = 275$ nm and $\lambda_{ex} = 295$ nm, respectively.

The increasing concentration of VIN and 5-FU in HSA–VIN and HSA–5-FU solutions produce an absorbance ≥0.05, thus intensity of recorded fluorescence was corrected with inner filter effect according to the following equation [5]:

$$RF_{cor} = RF_{obs} \times 10^{\frac{A_{ex}+A_{em}}{2}} \tag{1}$$

where: RF_{cor} and RF_{obs} show the relative fluorescence intensity corrected and observed; A_{ex} and A_{em} present the absorbance at excitation (A_{ex}) and emission (A_{em}) wavelength.

3.4. Absorption analysis. UV-absorption spectra were obtained on a spectrophotometer JASCO model V-530 using quartz cells 1 cm × 1 cm × 4 cm. Compensation error of apparatus for wavelength (λ) is equal to ± 1 nm and for absorbance (A) ± 0.00001. UV spectra were recorded in the range from 220 nm to 400 nm. Absorbance of the ligand at 280 nm, 295 nm and at the respective emission wavelength was used to inner filter correction. Absorbance at 280 nm was used for the comparative analysis of VIN/5-FU DPPC/VIN, DPPC/5-FU and DPPC/VIN/5-FU [4, 6].

4. Molecular modeling studies

Molecular modeling experiment were performed and graphically elaborated using the Molegro Virtual Docker (MVD) computer program version 2008.3.0. Molegro ApS.

4.1. Preparation of the target protein structure. The crystal structure of the HSA was downloaded to the MVD from the Protein Data Bank (PDB) with 4-letter PDB key: 1AO6 [7]. Loaded PDB file 4K2C contains two single, unglycosylated and ligand free polypeptide chains, A and B. The chain A was chosen as a target protein structure. Before experiment all water molecules were removed from the workspace. The chemistry of the target protein structure was automatically corrected to the physiological conditions. The polar amino acid

residues were protonated (His, Arg, Lys) or deprotonated (Asp, Glu) according to their protonation states at pH 7.4.

4.2. Physico-chemical properties of VIN and 5-FU molecules. The molecular descriptors for studied ligands were calculated using MarvinSketch computer program version 6.2.0. (ChemAxon Software Inc.) (Table 1). In aqueous solutions at physiological pH value basic molecule of VIN exists as a cationic form (78.85%), but acidic molecule of 5-FU mainly exists as a neutral form (69.73%). The value of partition coefficient at pH 7.4 (Log $D_{7.4}$) is relatively higher for VIN than 5-FU (Table 1). The MVD software was used for the pre-docking procedure of identification of the possible binding groups (template groups) in neutral molecule of 5-FU and ionized molecule of VIN (Table 2).

4.3. Detection of the potential binding sites in HSA structure. Potential binding sites in HSA structure (hereafter referred to as cavities, CAVs) were automatically detected by guided differential evolution search algorithm (DE) used in the MVD [8]. Then CAVs were segregated according to their molar volumes. CAVs with a molar volume greater than 100 Å^3 were selected as a proposed binding sites for ligands.

4.4. Molecular docking simulations. The final procedure of molecular modeling was molecular docking. Computational simulations were performed in MVD with standard docking parameters. During the experiment 5-FU and VIN were inserted and matched into CAVs. Different orientations of ligands in CAVs (poses) were ranked in order from the highest to the lowest binding energy according to the values of docking scoring function (MolDock Score). Poses with the lowest values of MolDock Score (arbitrary units) were selected as a final solutions for molecular docking experiment [8, 9]:
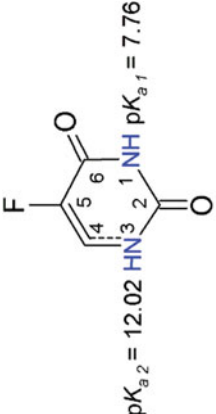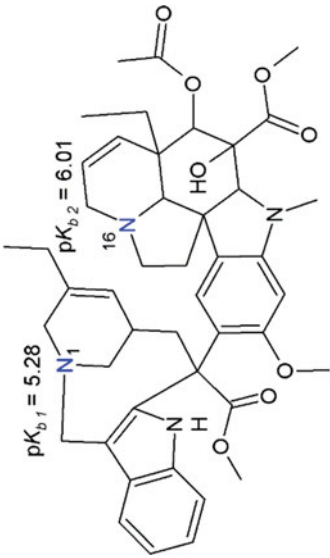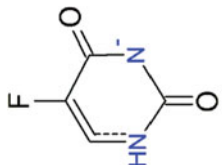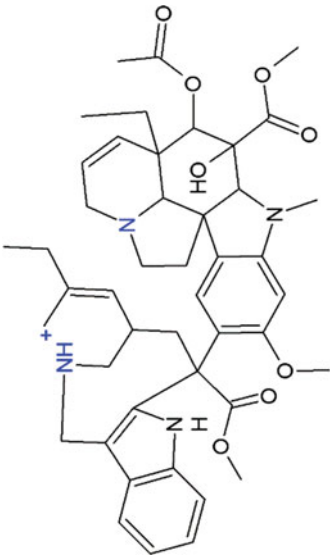
Results and Discussion

1. Encapsulation of 5-fluorouracil, Vinorelbine and the Mixture of Drugs to Liposomes

Encapsulation of drugs into liposomes formed from DPPC with cholesterol, prepared by mREV method, was confirmed by UV-Vis spectroscopy. UV-Vis absorption spectrum of DPPC liposomes containing 5-fluorouracil and vinorelbine encapsulated separately and together was compared with spectrum registered for supernatant remained after centrifugation of preparation mixture. Absorbance at 280 nm of the drugs encapsulated in liposomes (DPPC/5-FU, DPPC/VIN, DPPC/5-FU/VIN – 1.02, 1.11, 1.23) was compared with that of supernatant (0.23, 0.33, 0.51, respectively). We can state that majority of drug introduced into preparation mixture was encapsulated into liposomes.

The encapsulation efficiency is a measure of the percentage of the total compound entrapped within the liposome. In the liposome vesicles DPPC/5-FU and DPPC/VIN % of drug encapsulation amounts 94 % and 89% for 5-FU and VIN, respectively. DPPC/VIN/5-FU liposome containing both drugs contains 82 % of 5-FU and 56 % of VIN.
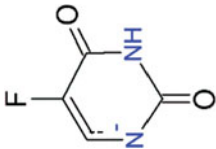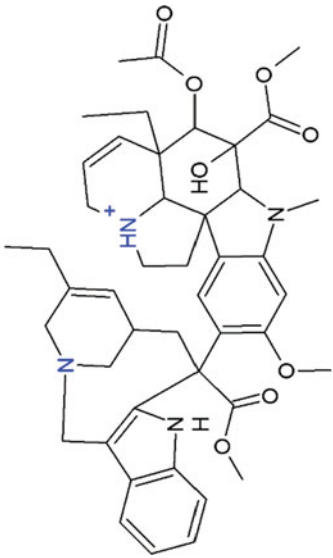
One can conclude that there is only a slight influence of VIN on the 5-FU encapsulation in liposome vesicle while 5-FU affects significantly the VIN content in the liposome vesicles.

Table 1. Ligands descriptors, dissociation constants and microspecies distributions at pH 7.4.

5-FU (weak acid)

VIN (weak base)

pK_{a1} = 7.76
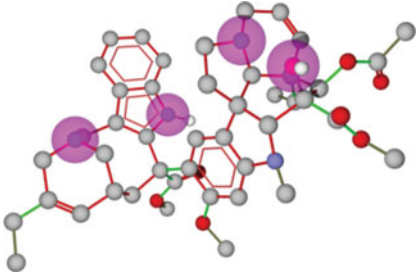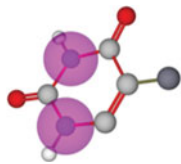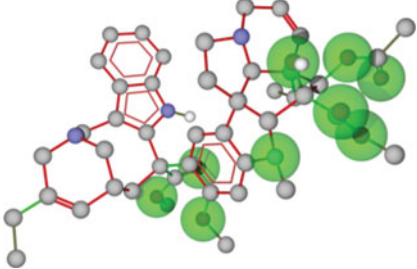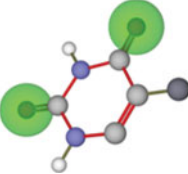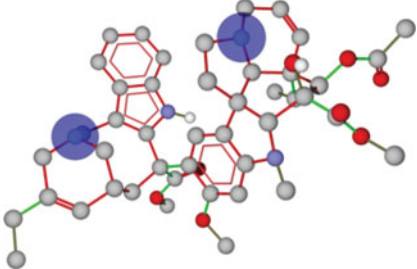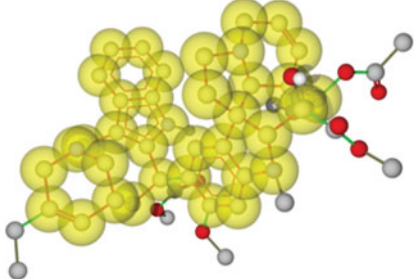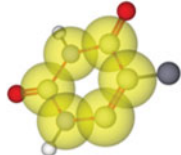
pK_{a2} = 12.02

69.73 %

29.04 %

pK_{b2} = 6.01

pK_{b1} = 5.28

0.96 %

15.13 %

Table 1. Ligands descriptors, dissociation constants and microspecies distributions at pH 7.4. (*Continued*)

5-FU (weak acid)	VIN (weak base)

1.23 %

5.04 %

78.85 %

Descriptor	5-FU	VIN
Molecular Weight (Da)	130.08 0	778.93
Molar Volume (Å^3)	93.61	715.84
Partition coefficient:		
Log $D_{7.4}$	– 1.00	– 2.63
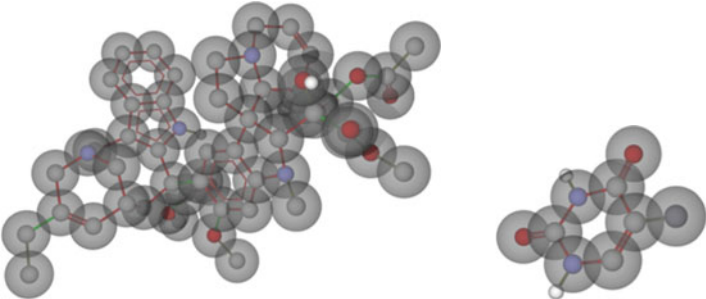
Log $D_{7.4}$ – octanol/water partition coefficient at pH 7.4. All the predicted values were generated using the MarvinSketch computer program.

Table 2. Visualization of template groups obtained for 5-FU and VIN with use of MVD.

Docking Template	Vinorelbine (VIN)	5-Fluorouracil (5-FU)
Hydrogen Donor (HD)		
Hydrogen Acceptor (HA)		
Positive Charge (PC)		
Rings Center (RC)		

Table 2. Visualization of template groups obtained for 5-FU and VIN with use of MVD. *(Continued)*

Docking Template	Vinorelbine (VIN)	5-Fluorouracil (5-FU)
Steric Area (SA)		

Atoms are colored by element (CPK): H – white, C – gray, O – red, N – blue and F – slate. Flexible bonds are colored green. Only polar hydrogens are shown.

2. *Determination of Phase Transition Temperature (T_c) in Liposomes*

With the increase of temperature the phase transition takes place in phospholipid membranes [10, 11]. Apart from the main phase transition between ripple gel phase and liquid-crystalline phase, two other phase transitions between lamellar, tilted and ripple phases can be determined [12]. In our previous studies temperature of the phase transition in DPPC membrane 299 K was determined by DSC technique [12]. Temperature of phase transition of liposomes without any drug obtained at pH 7.4 was 314 K. When vinorelbine was closed into liposome, temperature of phase transition does not change. When 5-fluorouracil was closed into liposome, temperature increases to 316 K. The increase of phase transition temperature attests that 5-FU, in contrast to VIN that remains closed in the vesicle, incorporates to liposomal bilayer interacting with its phospholipid chains and making its stiffener. The increase of the phase transition temperature of liposomes containing 5-FU in comparison to the liposome without drug shows that a higher temperature should be demanded to release 5-FU from vesicle.

3. *Binding to Human Serum Albumin (HSA)*

3.1. Binding site of 5-FU in HSA. The HSA fluorescence excited at 275 nm and 295 nm was quenched by 5-FU at the molar ratio 5-FU:HSA from 1:1 to 32:1 by 15% and 20% , respectively (Fig. 1A). A hypsochromic shift of fluorescence emission maximum of HSA by 4 nm and 3 nm observed for excitation at 275 nm and 295 nm, respectively, means that microenvironment within the binding site in HSA becomes more polar in the presence of 5-FU. The comparison of the curves of HSA fluorescence quenching by 5-FU shows that 5-FU quenches HSA fluorescence more at λ_{ex} 295 nm than λ_{ex} 275 nm (Fig. 1A). It means, that tyrosyl residues are not involved in the interactions 5-FU with HSA. The quenching of HSA fluorescence is due to energy transition from Trp 214 to 5-FU. Probably 5-FU forms a "sandwich-type" complex between its pyrimidyne ring and aromatic side chain of Trp 214. The binding site for 5-FU may be located deeply in subdomain IIA (Sundlow's site I), where Trp 214 residue is found [13,14]. The binding evokes the increasing hydrophobicity
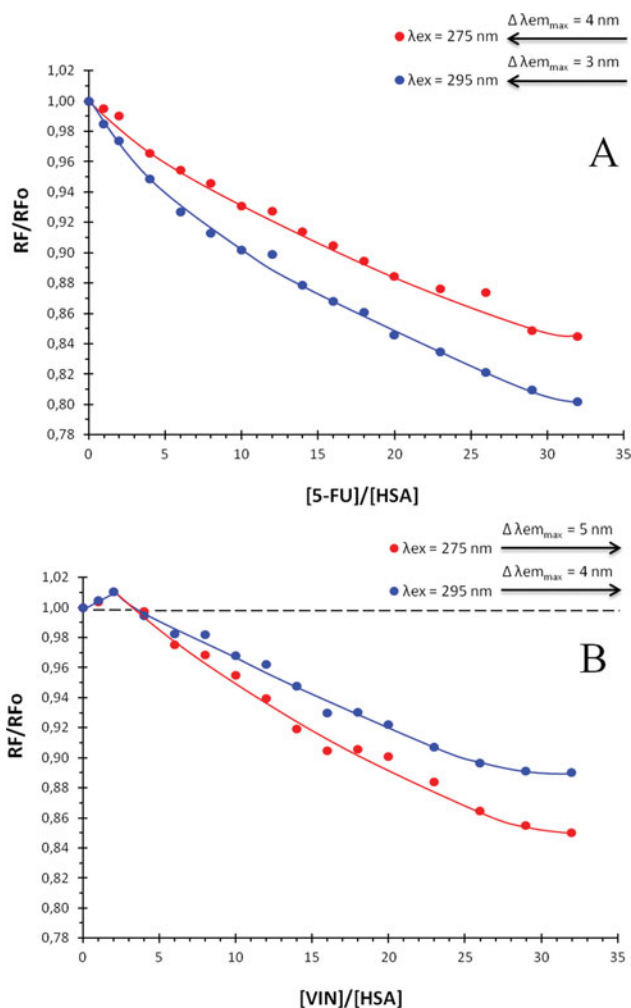
Figure 1. Quenching curves of HSA in the presence of 5-FU (A) and VIN (B) obtained for 275 nm and 295 nm excitation wavelenghts; HSA 1.0×10^{-6} M, VIN and 5-FU 1.0×10^{-6} M to 3.2×10^{-5} M.

in subdomain IIA resulting in the hypsochromic shift of the maximum fluorescence of HSA.

3.2. Binding site of VIN in HSA. The study of HSA fluorescence quenching by VIN shows that VIN at the molar ratio VIN:HSA from 1:1 to 3:1 causes a slight increase of fluorescence of HSA excited at both 275 nm and 295 nm (Fig. 1B). Only at a higher molar ratio, i.e. from 5:1 to 32:1, VIN quenches by 11% and 15% the fluorescence of HSA excited at 275 nm and 295 nm, respectively (Fig. 1B). It was accompanying by a bathochromic shift by 5 nm. The initial growth in fluorescence of HSA for molar ratio VIN:HSA smaller than 5:1 may be caused by the partial exposure of HSA fluorophores on the protein surface to limited contact with water molecules (Fig. 1B). The bathochromic shift of fluorescence emission maximum of HSA confirms above assumption, because it indicates an increase
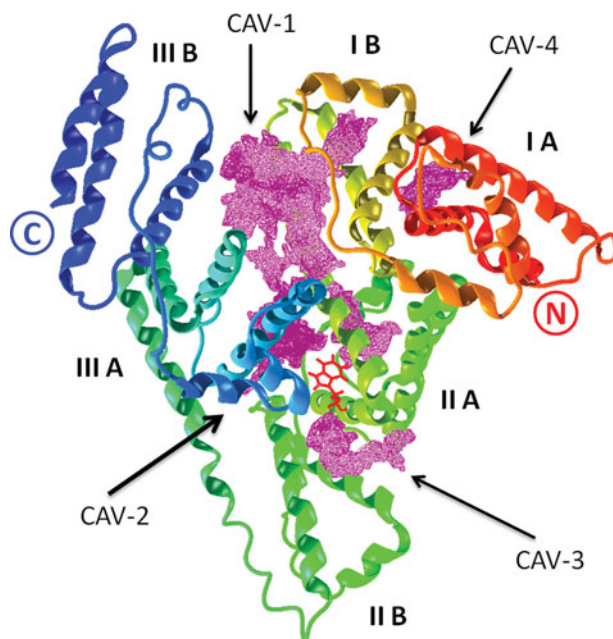
Figure 2. X-ray structure of HSA (PDB ID: 1AO6) represented by the ribbon model with the binding sites for drugs (CAVs) detected by MolDock. Each subdomain is vizualised with a different color according to the model proposed by Carter and Ho [13]: red for subdomain IA, orange for IB, bright green for IIA, dark green for IIB, cyan for IIIA and dark blue for IIIB. N- and C- termini are red and dark blue, respectively. CAVs are shown as a purple mesh. Trp214, which is likely to interact with 5-FU and/or VIN is depicted in red stick.

in polarity of microenvironment of fluorophores at the binding site of VIN. Quenching of HSA fluorescence for molar ratio VIN:HSA higher than 5:1 testifies about the possibility of energy transfer from HSA fluorophores to VIN molecule. VIN quenches fluorescence of HSA excited at 275 nm more than at 295 nm (Fig. 1B). This allows for a suggestion that both tryptophanyl and tyrosyl residues take part in the interactions with VIN. It is possible, that the VIN molecule may interact with these amino acid residues via the hydrogen bonding and electrostatic interactions in subdomain IIA (Sudlow's site I), where Trp 214 and Tyr 263 are located [13, 14].

3.3. Virtual screening of drug binding sites in HSA. As an introduction to molecular modeling four possible binding sites (CAVs), which represent the free space inside the HSA structure able to interactions with ligands, have been identified (Fig. 2). This CAVs can be filled by the molecule of different endogenous and exogenous compounds such as hormones, bilirubin, fatty acids, metal anions, warfarin, captopril and piroxicam [15–18]. Modeled sites were ranked in terms of molar volume and molecular surface (Table 3). The largest site, designated as CAV-1 is located partly on the protein surface between subdomains IB and IIIA and partly in hydrophobic core of HSA at subdomain IIIB. The second site, CAV-2 is found deep into the hydrophobic pocket of HSA and occupies the central core of the protein near Trp 214 residue. CAV-2 is located between four subdomains: IB, IIA, IIB and IIIA (mainly IIA). There are two small binding sites inside the hydrophilic pockets at the surface of HSA. CAV-3 is located between subdomain IIA and IIB, but CAV-4

Table 3. Volumes and surfaces of the top cavities in HSA molecule predicted by MolDock.

No.	Cavity	Molar volume (A^3)	Molar surface (A^2)
1	CAV-1	832.00	1928.96
2	CAV-2	451.07	1292.80
3	CAV-3	173.57	488.97
4	CAV-4	159.23	375.04

between subdomain IA and IB. Both 5-FU and VIN are large molecules (Table 1), therefore molecular docking experiments should be executed in CAV-1 and/or CAV-2. Based on the fluorescence quenching of HSA by 5-FU and VIN (Fig. 1A, B) it was concluded, that these ligands interact with HSA in CAV-2 near Trp 214 (subdomain IIA).

In this experiment CAV-2 was selected as a proposed binding site for docking of 5-FU and VIN. This cavities is surrounded by 58 amino acid residues within a radius of 6 Å. The entrance of the CAV-2 has a strong hydrophilic character, since it is surrounded by charged amino acids. At the entrance to the CAV-2 four acidic amino acids (Glu 153, Glu 188, Glu 292, Glu 294) and five basic amino acids (Lys 144, Lys 190, His 288, Lys 436 and Lys 444) are located. The interior of CAV-2 is negatively charged, because there are four acidic (Asp 23; Glu 153, Glu 199, Asp 340) and only two basic amino acids (Arg 218; Arg 222). There are positively charged Lys 195 and Lys 199 in balance with negatively charged Glu 450 and Glu451 at the bottom of CAV-2. The internal microenvironment of CAV-2 is dominated by hydrophobic residues, mainly alanine (Ala 194, Ala 210, Ala 215, Ala 291, Ala 448, Ala 449), leucine (Leu 198, Leu 203, Leu 345, Leu 347, Leu 453, Leu 481) and valine (Val 293, Val 343, Val 344, Val 455, Val 456, Val 482). Aromatic residues at positions Phe 211, Trp 214, Tyr 341 and Tyr 452 create the bottom of CAV-2. These results of molecular modeling of the drugs binding sites in HSA structure are consistent with the data found for piroxicam, 6-mercaptopurine and saturated fatty acids [16, 17, 19].

3.4. Visualization of 5-FU complex with HSA (5-FU–HSA complex). The neutral molecule of 5-FU was closely matched to the hydrophobic pocket of CAV-2 as a result of computer simulation (Fig. 3A). The relatively lipophilic nature of un-ionized 5-FU molecule (Table 1) make easier the formation of steric interactions with HSA in a non-polar microenvironment at the bottom of CAV-2 (MolDock $_{energy} \sim -61.9$ a. u.). 5-FU is surrounded within a radius of 3 Å by some aliphatic side chains of leucine (Leu 198, Leu 347, Leu 481, Leu 482) and a valine (Val 344) (Fig. 4A). Probably these residues may contact with unionized 5-FU only by the van der Waals interactions. This complex can be stabilized by π-π stacking interactions between pyrimidine ring of 5-FU and aromatic ring of Trp 214. 5-FU may interact also with aromatic ring Tyr 341 and/or Tyr 452. A "sandwich-type" complex of 5-FU formed with Trp 214 is proposed and visualized on Fig. 4A.

3.5. Visualization of VIN complex with HSA (VIN–HSA complex). Within a radius of 3 Å from docked VIN molecule there were only three hydrophobic amino acids, that may contact with VIN by the van der Waals interaction, Val 293, Val 343 and Cys 448 (Fig. 4B). The indole and pyrimidine rings of VIN may form a "sandwich-type" complex with aromatic rings of Trp 214, Tyr 341 and/or Tyr 452 by π-π interaction (MolDock $_{energy} \sim -15.9$ a. u.) (Fig. 4B). Results of docking of VIN to CAV-2 showed, that hydrogen
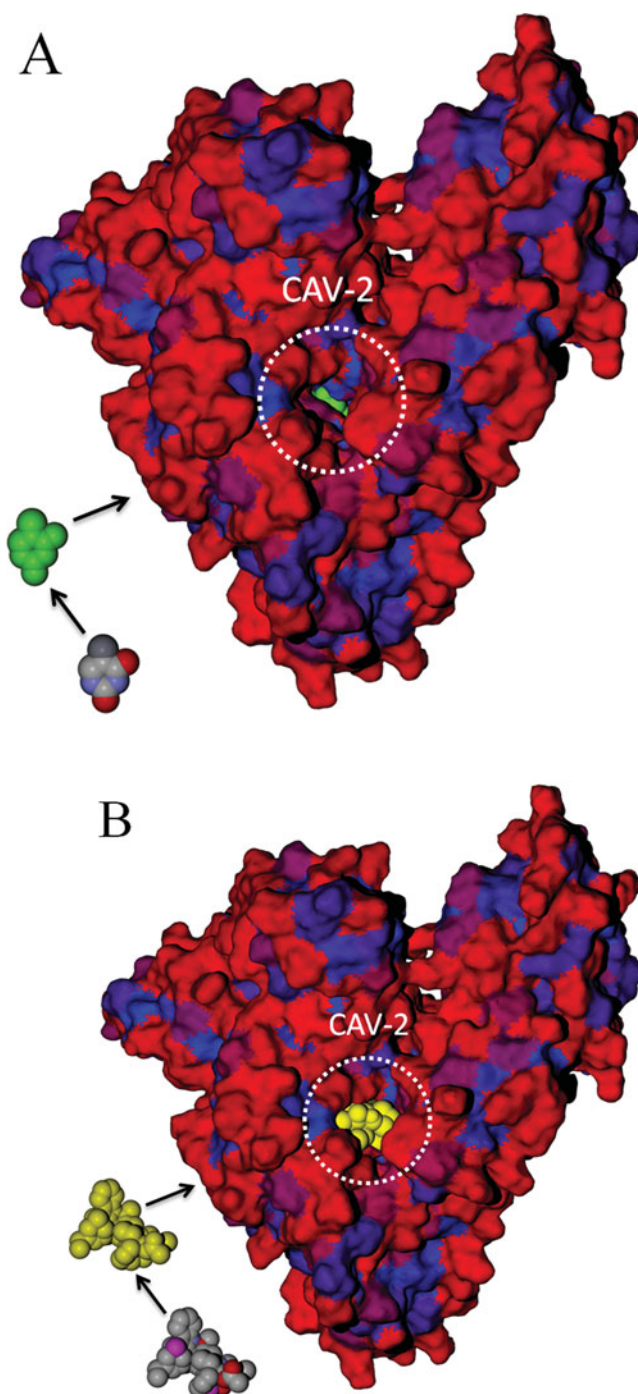
Figure 3. Computer docking of 5-FU (A) and VIN (B) into the binding site 2 (CAV-2) located between subdomains II A, IIB and IIIA in the native molecule of HSA [7]. Molecular surface of the protein is colored according to the hydropathy index proposed by Kyte and Doolittle [20]: red and blue for the most hydrophilic and hydrophobic areas, respectively. CAV-2 is marked with a circle. Ligands are presented as a spacefil model (the van der Waals radius of each atom is used as radius for the sphere). 5-FU is colored green, VIN is colored yellow.
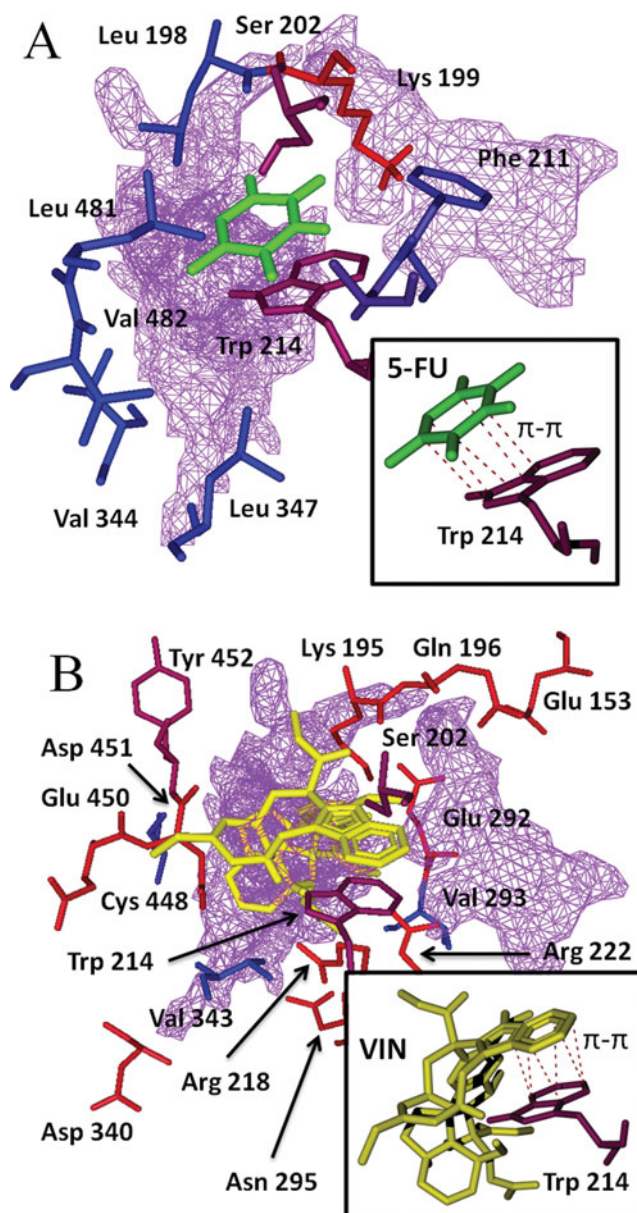
Figure 4. Docking views showing the best binding orientations (poses) and steric interactions of 5-FU (A) and VIN (B) with HSA. The free space of the CAV-2 between HSA residues is shown as purple mesh. Amino acids, which are capable of forming the steric interaction with 5-FU and/or VIN are displayed in a color scale from red for polar amino acids to blue for non-polar amino acids [20]. 5-FU is colored green, VIN is colored yellow. Possible π-π stacking interactions are depicted in dotted red lines. All non-polar hydrogens were hidden for clarity. Picture were generated using the MVD.
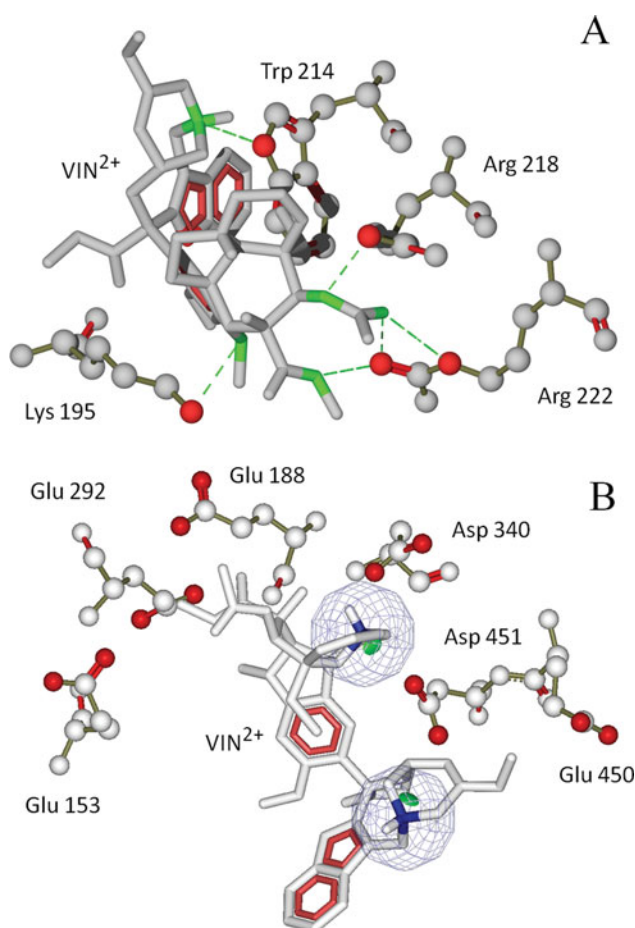
Figure 5. The model of hydrogen bonding (A) and electrostatic interactions (B) between VIN and HSA. (A): hydrogen bonds (HB) are visualized in dashed green lines; atoms are colored red for HB donors and green for HB acceptors. (B): strong and favorable electrostatic interactions are visualized as a green partial spheres oriented in the direction of interaction; electron density maps of NH^+ groups in pyridine rings of VIN are shown as blue wire spheres; atoms are colored blue for positive charge or red for negative charge. Amino acids are visualized in ball and stick graphical style. VIN is represented by stick model. Only polar hydrogens are shown. Pictures were generated using the MVD.

bonding are responsible for the creation of VIN–HSA interaction (Fig. 5A). There were three strong hydrogen bonds (MolDock $_{energy}$ $\sim$ $-$ 2.5 a.u.) with Lys 195, Arg 218 and Arg 222 (distance $\sim$ 2.6 Å). It was also found a semi-strong hydrogen bond (MolDock $_{energy}$ $\sim$ $-$ 1.5 a. u.) with Arg222 (distance $=$ 3.1 Å) and two weak hydrogen bonds (MolDock $_{energy}$ $\sim$ $-$ 0.5 a. u.) with Trp 214 and Arg 222 (distance $=$ 3.1 Å). VIN-HSA complex is stabilized by electrostatic interactions (Fig. 5B) between NH^+ group of VIN and negatively charged amino acids. MVD allows for identification of two strong (distance $<$ 4.5 Å) electrostatic interaction with Asp 451 (MolDock $_{energy}$ $\sim$ $-$ 2.5 a. u.) and five weak electrostatic interaction (distance $>$ 4.5 Å) with Glu 153 (MolDock $_{energy}$ $\sim$ $-$ 0.6 a. u.), Glu 188 (MolDock $_{energy}$ $\sim$ $-$ 0.3 a. u.), Glu 292 (MolDock $_{energy}$ $\sim$ $-$ 1.3
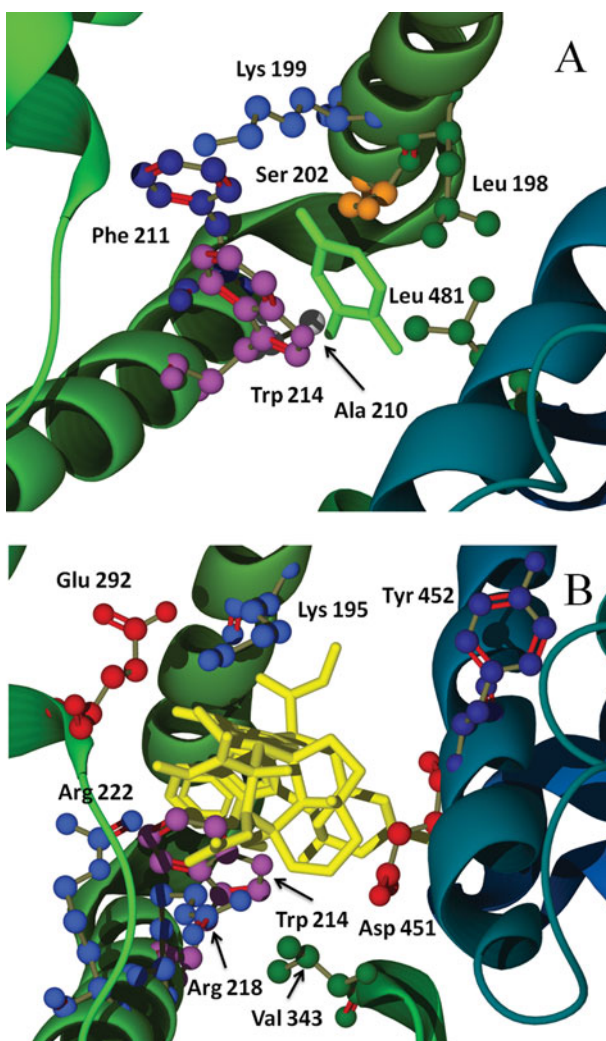
Figure 6. The comparison of docking results obtained for process of binding of 5-FU (A) and VIN (B) to CAV-2 in HSA molecule. Selected fragments of HSA tertiary structure are visualized as an α-helices colored green for subdomain IIA and cyan for subdomain IIIA. Amino acids capable of interacting with 5-FU and VIN are visualized in ball and stick style and colored by their type: acidic are red (Asp, Glu), basic are blue (Arg, Lys), aliphatic are white (Ala) or green (Leu, Ile), aromatic are dark blue (Phe) or violet (Trp, Tyr) and hydroxyl-containing are orange (Ser). Ligands are shown as a green and yellow stick models for 5-FU and VIN respectively. All hydrogens were hidden for clarity. Docking results were obtained using the MolDock.

a. u.), Asp 340 (MolDock $_{energy}$ ∼ − 0.7 a. u.) and Glu 450 (MolDock $_{energy}$ ∼ − 1.7 a. u.). These models of interaction obtained for VIN–HSA complex and 5-FU–HSA complex are in agreement with template groups in 5-FU and VIN, respectively (Table 2). The final solution of docking procedure was shown in Fig. 6A, B.

Conclusions

We proposed the modified reverse-phase evaporation method (mREV) to prepare liposomes able to transport vinorelbine and 5-fluorouracil, anticancer drugs that are used in multidrug therapy of cancer. Encapsulation of vinorelbine does not affect phase transition temperature (Tc) value in comparison with the liposomes formed without the drug. Temperature (Tc) increases for liposomes containing 5-fluorouracil. Analysis of competition in the encapsulation of 5-fluorouracil and vinorelbine shows that 5-FU incorporates in more extend to liposomes than VIN and affects the temperature of phase transition (Tc) of phospholipide forming liposomal membrane. There is only a slight influence of VIN on the 5-FU encapsulation in liposome vesicle while 5-FU affects significantly the VIN content in the liposome vesicles.

The fluorescent analysis and the molecular docking have been applied to explain the binding mechanism of 5-FU and VIN to HSA. Based on the fluorescence analysis it was concluded that VIN and 5-FU bind both to HSA in subdomain II A, near Trp 214 residue. The 5-FU molecule penetrates deep into the hydrophobic interior of subdomain IIA, while VIN molecule is partially bound on the protein surface and exposed to a more hydrophilic environment of HSA. In summary, the tryptophanyl residue (Trp 214) plays a key role in the binding of 5-FU and VIN to HSA. Fluorescent studies have been confirmed by the results of computer simulation. Docking results suggested, that the binding of VIN molecule to HSA is probably stronger than that of 5-FU molecule, because is enhanced by hydrogen bonds with Lys 195, Arg 218, Arg 222 and electrostatic interaction with Asp 451. This can explain a fact that 5-FU encapsulates easier in liposomal bilayer than VIN and that temperature of phase transition for DPPC/5-FU is higher than for DPPC liposome.

Funding

References

[1] Drummond, D. C., Noble, C. O., Guo, Z., Hayes, M. E., Park, J. W., Ou Ching-Ju, Tseng Yun-Long, Hong, K. & Kirpotin, D. B. (2009). *J. Pharmacol. Exp. Ther.*, *328*, 321.

[2] Semple, S. C., Leone, R., Wang, J., Leng, E. C., Klimuk, S. K., Eisenhardt, M. L., Yuan Zuan-Ning, Edwards, K., Maurer, N., Hope, M. J., Cullis, P. R. & Ahkong Quet-Fah. (2005). *J. Pharm. Sci.*, *94*, 1024.

[3] Sułkowski, W. W., Pentak, D., Korus, W. & Sułkowska, A. (2005). *Spectrosc. Int. J.*, *19*, 37.

[4] Równicka-Zubik, J., Czopek, I., Hartabus, A., Zawada, Z., Maciążek-Jurczyk, M., Szkudlarek-Haśnik, A., Sułkowska, A., Kos, A., Żądło, M. & Sułkowski, W.W. (2012). *Mol. Cryst. Liq. Cryst.*, *555*, 218.

[5] Elfaramawy, S. M. & Rizk, R. A. (2011). *J. Am. Sci.*, *7*, 365.

[6] Lakowicz, J. R. (2006). *Principles of Fluorescence Spectroscopy, third ed.*, Springer: New York, USA.

[7] Sugio, S., Kashima, A., Mochizuki, S., Noda, M. & Kobayashi, K. (1999). *Protein Eng.*, *12*, 439. (http://www.rcsb.org/pdb/explore.do?structureId = 1ao6)

[8] Thomsen, R. & Christensen, H. (2010). *J. Med. Chem.*, *49*, 3315.

[9] Molegro ApS. (2008). *Molegro virtual docker, user manual*.

[10] Urban, E. & Bota, A. (2005). *J. Therm. Anal. Cal.*, *82*, 463.

[11] Hatta, I. (2005). *J. Therm. Anal. Cal.*, *82*, 189.

[12] Pentak, D., Sułkowski, W.W. & Sułkowska, A. (2008). *J. Ther. Anal. Cal.*, *93*, 471.

[13] Carter, D. C. & Ho, J. X. (1994). *Adv. Protein Chem.*, *45*, 153.

[14] Sudlow, G. (1975). *Mol. Pharmacol.*, *11*, 824.

[15] Otagiri, M. (2005). *Drug. Metab. Pharmacokinet.*, *20*, 309.

[16] Równicka-Zubik, J., Sułkowski, L., Maciążek-Jurczyk, M., Sułkowska, A. (2013). *J. Mol. Struct.*, *1044*, 152.

[17] Petitpas, I., Grune, T., Bhattacharya, A. A., Curry, S. (2001). *J. Mol. Biol.*, *314*, 955.

[18] Dockal, M., Chang, M., Carter, D. C., Ruker, F. (2000). *Protein Sci.*, *9*, 1455.

[19] Sochacka. J., Sobczak, A., Pawełczak, B. (2011) *Ann. Acad. Med. Siles.*, *65*, 41.

[20] Kyte, J. & Doolittle, F. (1982). *J. Mol. Biol.*, *157*, 105.